

Hyperfine Structure of the $6s6p\ ^1P_1$ Level of the Stable Ytterbium Isotopes*

B. Budick[†] and J. Snir

The Hebrew University, Jerusalem, Israel

(Received 8 August 1968)

The techniques of level-crossing and anticrossing spectroscopy have been applied in a study of the hfs of the excited $6s6p\ ^1P_1$ level of the stable ytterbium isotopes. Details concerning the anticrossing signal, its nature, shape, intensity, and dependence on polarized light are given. The values we infer for the hfs constants are $A(^1P_1)/g_J = 206.0(16)$ Mc/sec for Yb^{171} ($I = \frac{1}{2}$) and $A(^1P_1)/g_J = 56.9(5)$ Mc/sec, $B(^1P_1)/g_J = 575(7)$ Mc/sec for Yb^{173} ($I = \frac{5}{2}$). The measured values for the 1P_1 level are compared with those calculated from the known hfs constants of the 3P_1 and 3P_2 levels. Fair agreement is obtained with predictions based on the modified Breit-Wills theory given by Lurio.

INTRODUCTION

The hyperfine structure (hfs) of the $6s6p\ ^1P_1$ level of the ytterbium (Yb) atom has received considerable attention from optical spectroscopists. The hfs constants of Yb^{173} have been measured by Ross and Murakawa¹ who found $A = 1.3$ mK and $B = 23.2$ mK and by Gerstenkorn² whose preliminary results are $A = 3 \pm 1$ mK and $B = 19 \pm 3$ mK. For both values of the ratio B/A , the $F = \frac{5}{2}$ level is predicted to be inverted much below the $F = \frac{7}{2}$ and $F = \frac{3}{2}$ levels. However, the ratio deduced from Ross and Murakawa's result implies that the $F = \frac{7}{2}$ level is inverted as well and lies below the $F = \frac{3}{2}$ level. Gerstenkorn's result leaves the $F = \frac{7}{2}$ level with the highest energy.

Interest in the 1P_1 level has also been generated by the appearance of a paper by Lurio³ which relates the hfs constants of 1P and 3P terms of an sp configuration in a modified Breit-Wills approach. We have recently completed precision measurements of the hfs constants in the 3P_1 level,⁴ using the level-crossing technique. A comparison with the constants from the 1P_1 level would provide a check on the modified Breit-Wills approach or possibly reveal the presence of important configuration interaction effects.

Further consideration of the problem revealed that the excitation of Zeeman sublevels of the inverted hfs states with resonance radiation would furnish, in addition to the normal level-crossing signals, a narrow anticrossing signal. This is apparent from Fig. 1. The level ordering in the figure is in agreement with Gerstenkorn's hfs constants for reasons given below. The third hfs level, $F = \frac{5}{2}$, has an energy of -540 Mc/sec and cannot be shown conveniently. The distance of closest approach between the anticrossing levels is given by $|2V|$ where V is the matrix element of the interaction coupling the base states $F = \frac{7}{2}$, $M_F = -\frac{3}{2}$ and $F = \frac{3}{2}$, $M_F = -\frac{3}{2}$. The anticrossing is especially sharp because there is no first-order perturbation between states with $\Delta F = 2$. Observable level crossings lie at higher and lower fields and are circled in the figure. The anticrossing signal has the advantage that it can be clearly separated from the more intense, overlapping level crossings by choosing particular polarizations for the exciting and emitted light.

The anticrossing signal has one other interesting

property which has been reported.⁵ Both Fig. 1 and more detailed calculations indicate that the F, M_F representation is valid in the region of interest, e.g., 0–70 G. A photon which is capable of exciting one of a pair of repelling levels must also excite the other member of the pair. Thus the levels are excited coherently and also decay coherently in much the same fashion as a level-crossing signal. This is in marked contrast to the first reported anticrossing signals⁶ in which the appropriate base states were labeled by m_I and m_J . In that case, two base states of the same $m = m_I + m_J = m_I' + m_J'$ could not be excited from the same Zeeman sublevel in the ground state since the selection rule $\Delta m_I = 0$ must hold in the excitation. The anticrossing observed in that case resembled a double resonance signal in that it was

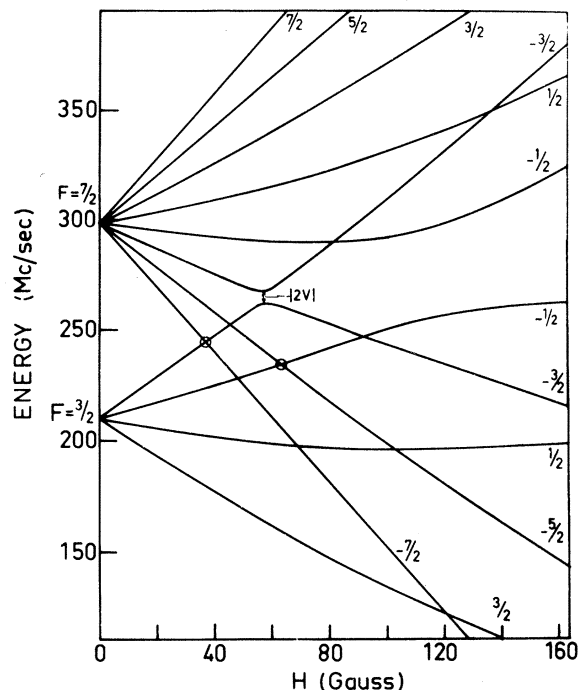


FIG. 1. Zeeman levels of the 1P_1 state of Yb^{173} . The $F = \frac{5}{2}$ state has an energy of -540 Mc/sec and is not shown. Observed level crossings are circled.

largest when only one of the excited base states was populated. The state mixing produced by the hfs dipole operator or by an external radio-frequency field is then responsible for a population redistribution resulting in an observable signal. The signals reported in this paper are largest when none of the electric dipole matrix elements describing the excitation and decay vanish.

Finally we note that as far as the actual physical levels are concerned, these are superpositions of the base states in the region of the anticrossing, and in this sense all anticrossing signals result from a coherent excitation. On the other hand, one may choose the point of view that all level crossings are really anticrossings since some perturbation, perhaps in n th order, will enter to push the levels apart. This repulsion will go undetected if the matrix element of the perturbation, V , is much smaller than the radiation width $\gamma = 1/2\pi\tau$, where τ is the lifetime of the state.

THEORY OF THE EXPERIMENT

Natural Yb contains 14% Yb^{171} ($I = \frac{1}{2}$) and 16% Yb^{173} ($I = \frac{5}{2}$). The hfs anomaly of the 3P_1 level has recently been measured.⁷ Knowledge of the hfs constant, A , for Yb^{171} in the 1P_1 level and of the recently measured nuclear magnetic moments⁸ immediately yields the corresponding constant for Yb^{173} . Our first experiments were therefore directed toward a measurement of A^{171} . The Zeeman effect for the 1P_1 level of the spin- $\frac{1}{2}$ isotope is shown in Fig. 2. The effect of the level crossing of the excited-state Zeeman sublevels (circled in the figure) on resonance radiation scattered by a sample of atoms has been treated by Franken.⁹ Briefly, when the magnetic field is varied so as to produce a degeneracy of the $F = \frac{3}{2}$, $M_F = -\frac{3}{2}$ and $F = \frac{1}{2}$, $M_F = -\frac{1}{2}$ levels, light linearly polarized perpendicular to the magnetic field can excite both levels coherently. The fluorescence to the $F = \frac{1}{2}$, $M_F = -\frac{1}{2}$ level of the ground state will then contain interference terms. The single level-crossing signal is sufficient to determine the ratio A^{171}/g_J since this ratio is related to the value of the crossing field, H_C , by the equation

$$A^{171}/g_J = \mu_0 H_C (1 + \frac{1}{2}g_I^{171}/g_J). \quad (1)$$

In this equation μ_0 is the Bohr magneton and g_I^{171} is the nuclear g factor taken as positive when the magnetic moment is negative. A value of $g_J = 1.05(2)$ has recently become available.¹⁰

The situation in Yb^{173} is considerably more complicated as can be seen from Fig. 1. In addition to the overlapping $\Delta m = 2$ level-crossing signals that are circled, there is a $\Delta m = 1$ level crossing between the levels $F = \frac{7}{2}$, $M_F = -\frac{5}{2}$ and $F = \frac{3}{2}$, $M_F = -\frac{3}{2}$ as well as the anticrossing signal. Eck has given a general expression for the resonance fluorescence signal, expressed as a function of Δ , the energy separation of the relevant energy levels:

$$S = (1/\gamma)\sum(|f_a|^2|g_a|^2) + (1/\gamma)\sum(|f_b|^2|g_b|^2)$$

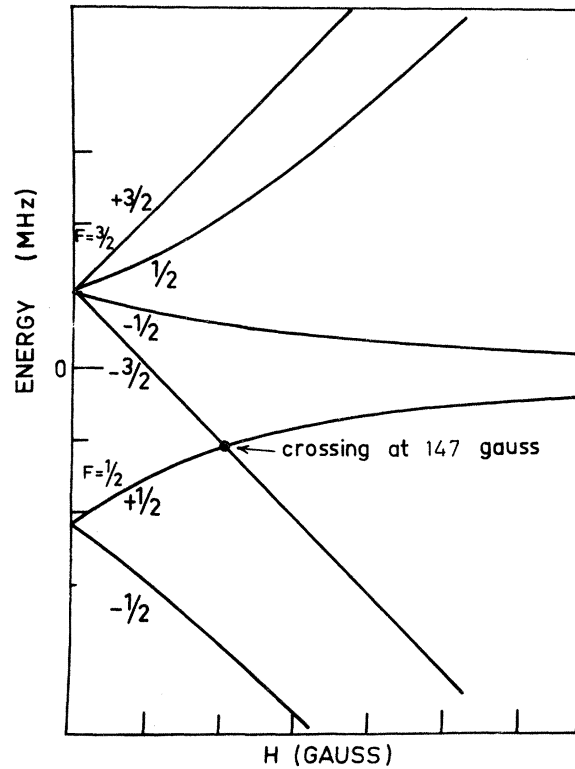


FIG. 2. Zeeman levels of the 1P_1 state of Yb^{171} . The observed level crossing is circled.

$$\begin{aligned} & + (2\gamma/D)\sum f_a f_b g_a g_b - (2|V|^2\gamma/D)\sum fg \\ & + (2V^2/\gamma D)\sum (2f_a f_b)(2g_a g_b) \\ & + (2V\Delta/D)\sum [f(g_a g_b) + g(f_a f_b)], \quad (2) \end{aligned}$$

where $D = \gamma^2 + |2V|^2 + \Delta^2$ is the resonance denominator,

$$f = (1/\gamma)(|f_a|^2 - |f_b|^2),$$

$$g = (1/\gamma)(|g_a|^2 - |g_b|^2),$$

and V is the matrix element of the perturbation which couples the base states a and b . The symbol f_a is used to represent the dipole matrix element $f_{am} = \langle a | \vec{r} \cdot \vec{r} | m \rangle$ that connects state a to the ground-state Zeeman level m . Similarly, $g_a = g_{m'a} = \langle m' | \vec{g} \cdot \vec{r} | a \rangle$ is the matrix element for the decay. The summations are carried out over all initial levels m and final levels m' involved in the excitation and decay. We have simplified Eck's original expression in obtaining Eq. (2) by noting that both levels have the same lifetime and that the perturbation V is real for the anticrossing. In addition, with the geometry given below, the matrix elements f_a , f_b , g_a , and g_b may all be chosen as real.

For the level-crossing signals $V=0$, and only the first three terms are nonvanishing. The res-

onance-type signals are due to the third term which requires coherence in both excitation and decay, i. e., none of the matrix elements may vanish. The fourth term is the pure anticrossing signal observed by Eck.¹¹ It is a maximum when one of the excitation matrix elements and/or one of the decay matrix elements vanishes. The fifth and sixth terms are mixed crossing and anticrossing terms that require coherence in at least one of the two steps of the resonance fluorescence process. Each of the last four terms in Eq. (2) makes a contribution to the anticrossing signal.

The matrix elements in Eq. (2) are between the base states that we choose to describe our system and not between the actual, physical states which are equal mixtures of the base states in the vicinity of the anticrossing and exhibit strong curvature there. The choice of base states is indicated by Fig. 1 which shows that all levels involved in crossing and anticrossing signals have hardly deviated from the straight-line behavior characteristic of the F, M_F representation. This is a consequence of the fact that neither the hfs interaction nor the magnetic field couples states with $\Delta F=2$ in first order. The perturbation V is, in fact, provided by a second-order magnetic field perturbation via the $F=\frac{5}{2}, M_F=-\frac{3}{2}$ level. Since this level is far removed in energy from the anticrossing levels, the perturbation V is small, permitting the observation of sharp signals.

With the base states chosen as $|a\rangle = |\gamma, F, M_F\rangle$, etc., and assuming the incident light to be propagating in the y direction with the magnetic field in the z direction, we may evaluate the maximum intensity of all crossing and anticrossing signals for the experimental geometry given below. When polarized light is used, the angles between the direction of polarization and the z direction for the incident and scattered light are denoted by θ_1 and θ_2 , respectively. With the aid of the matrix elements given in Table I, the intensities and angular dependences listed in Table II were obtained. For completeness the line shapes determined by an inspection of Eq. (2) are also given. The intensities given in Table II do not include corrections for the relative linewidths of the signals which, for example, modifies the intensity ratio of the $\Delta m=2$ to $\Delta m=0$ signals to approximately 8 : 1. Perhaps the most striking aspect of Table II is the very different dependence of the different types of signals on polaroid orientation. The manner in which this difference was exploited experimentally is given in detail below in the section entitled Experimental Procedure and Results.

TABLE I. The dipole matrix elements connecting the ground state 1S_0 with the anticrossing levels in the 1P_1 excited state.

F, M_F	1S_0		
	$\frac{5}{2}, -\frac{1}{2}$	$\frac{5}{2}, -\frac{3}{2}$	$\frac{5}{2}, -\frac{5}{2}$
$\frac{7}{2}, -\frac{3}{2}$	$(5/21)^{1/2}(\hat{i}-\hat{j})$	$(10/21)^{1/2}\hat{k}$	$-(1/42)^{1/2}(\hat{i}+\hat{j})$
$\frac{3}{2}, -\frac{3}{2}$	$-(1/30)^{1/2}(\hat{i}-\hat{j})$	$(4/15)^{1/2}\hat{k}$	$(1/3)^{1/2}(\hat{i}+\hat{j})$

EXPERIMENTAL TECHNIQUE AND APPARATUS

The technique used in the present experiments is primarily that of level-crossing spectroscopy. Resonance radiation, corresponding to the transition $(6s)^2\ ^1S_0 \rightarrow 6s6p\ ^1P_1$ at 3987 Å was incident on a dense atomic beam of Yb. The hollow cathode in the light source was machined from a cylinder of natural Yb. The atomic vapor that served to scatter the resonance radiation was produced by an oven capable of being heated by electron bombardment. The dense atomic-beam apparatus has been described elsewhere.¹² Vapors of natural Yb and of samples enriched in Yb¹⁷³ were used in the experiments. In practice, it was found that approximately 40 W of power delivered to a 6.5-mil tungsten wire surrounding the oven were sufficient to produce a usable density, and electron bombardment was unnecessary. Ovens of molybdenum and of tantalum were used successfully. Light scattered at 90° to both the incident light beam and to the magnetic field passed through a narrow band interference filter peaked at 4000 Å and into a photomultiplier (EMI 6256 B).

The magnetic field was produced in the 3-in. gap of a 12-in. Harvey-Wells electromagnet. Additional windings on the pole faces provided a modulating field at 28 cps. Proton NMR served to measure magnetic fields in excess of 130 G. For purposes of measuring lower fields, a Hall-effect probe was calibrated with proton resonance before and after each run.

Incident and scattered light was polarized with the aid of Polacoat PL 40 MR polarizers. These polarizers are intended for the near ultraviolet but they are also excellent in the 4000 Å region. They could be mounted in rotatable holders whose axis could be read with respect to a fixed protractor. Settings were reproducible to a few degrees.

TABLE II. Shape, intensity, and angular dependence of terms contributing to the crossing and anticrossing signals.

Signal	Term	Intensity \times $(\gamma^2 + 2V ^2)^{-1}$	Angular dependence	Line shape
$\Delta m=2$	3	9.67	$\sin^2\theta_1 \sin^2\theta_2$	absorption
$\Delta m=1$	3	5.53	$\sin 2\theta \sin 2\theta_2$	absorption
$\Delta m=0$	3	1.84	$(3 \cos^2\theta_1 - 1)(3 \cos^2\theta_2 - 1)$	absorption
	4	-0.01	$(3 \cos^2\theta_1 - 1)(3 \cos^2\theta_2 - 1)$	absorption
	5	0.08	$(3 \cos^2\theta_1 - 1)(3 \cos^2\theta_2 - 1)$	absorption
	6	0.23	$(3 \cos^2\theta_1 - 1)(3 \cos^2\theta_2 - 1)$	dispersion

EXPERIMENTAL PROCEDURE AND RESULTS

In the first experiments a vapor of natural Yb served to scatter the unpolarized resonance radiation. The scattered light was also unpolarized. Very strong signals were observed at zero magnetic field, corresponding to the Hanle effect or zero-field level crossings. As the field was increased, weak level-crossing signals were observed in the vicinity of 40 G and a single strong signal appeared at approximately 147 G. Attempting to identify the signals, we substituted a sample of Yb enriched to 85% in Yb^{173} and containing only 0.7% Yb^{171} in our atomic-beam oven. The strong signal vanished and could therefore be attributed to Yb^{171} .

On the other hand, the signals in the vicinity of 40 G were now much enhanced. These signals, as noted above, are superpositions of $\Delta m = 2$, $\Delta m = 1$, and $\Delta m = 0$ crossings and anticrossings with intensities and dependences on polaroid orientation as given in Table II. From the table it is apparent that for π light ($\theta = 0$), the function $3 \cos^2 \theta - 1$ is a maximum while $\sin 2\theta$ and $\sin^2 \theta$ both vanish. Figure 3 was obtained with π light in both the incident and detection channels of the apparatus. Sharp anticrossing signals appear at ± 56.1 G. The dispersion-type line shape is a consequence of the lock-in detection used in our experiment. Thus the integrated line shape is that of an absorption curve with perhaps a small dispersion-type admixture in agreement with the predictions of Table II. Any precise determination of the signal asymmetry and of the dispersion-curve content in the signal is ruled out because of perturbations from the nonresonant background, from the anticrossing at negative (positive) magnetic field, and possibly from the anticrossing of the $M = -\frac{1}{2}$ levels shown in Fig. 1.

Assuming that the signal is perfectly symmetric (the predicted asymmetry is of the same order as that produced by a slight misalignment of our optics), we find that the peak-to-peak separation is given by⁶

$$\delta_P = (2/\sqrt{3})(\gamma^2 + |2V|^2)^{1/2}. \quad (3)$$

A value of $\gamma = 29.0$ Mc/sec can be inferred from the measured lifetime of the 1P_1 level.¹³ For $2V$ we may take the distance of closest approach shown in Fig. 1 of 6.3 Mc/sec. This leads to a prediction of 22.9 G for δ_P where the calculated slope 1.51 Mc/Gsec has been used as a conversion factor. The value found from a succession of curves, in which the density of scattering atoms was reduced to eliminate coherence narrowing,¹³ is 22.5 ± 1.0 G.

A pure $\Delta m = 2$ level-crossing curve may be obtained with the incident (or detected) light linearly polarized at an angle of 55° to the magnetic field while the detected (or incident) light is unpolarized. The anticrossing signal vanishes for this orientation while the $\Delta m = 1$ signal vanishes for unpolarized light. With this choice of polarization Fig. 4 was obtained. Besides the Hanle effect or zero-field level crossing, one easily observes a second strong crossing at approximately ± 35 G and, with somewhat greater difficulty, a third crossing at approximately ± 60 G. When corrected for overlap, the strong crossing is found to lie at 36.2 ± 1.0 G. That this is in excellent agreement with the field found for the anticrossing can be shown from a simple calculation based on the g_F factors. The ratio of anticrossing to crossing fields is easily predicted to be $\frac{14}{9}$. The observed intensity of the crossing signal was observed to be between 5 and 10 times as great as that of the anticrossing signal in agreement with the discussion given earlier.

A curious, and at first inexplicable, curve was obtained when both the resonance radiation and the fluorescence were linearly polarized at 55° . The curve is shown in Fig. 5. It is asymmetric about zero magnetic field and evidently contains a signal which reverses sign with magnetic field direction. This is just the behavior predicted for

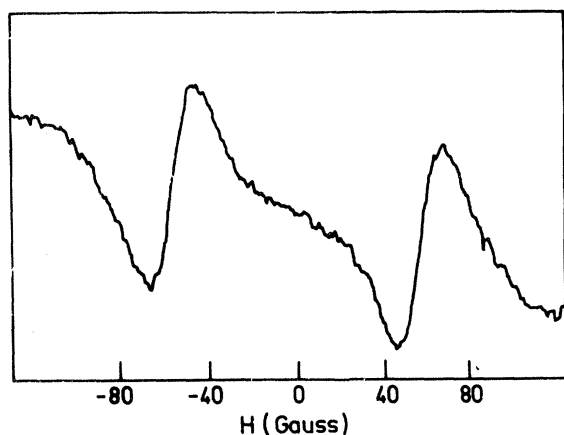


FIG. 3. Anticrossing signals observed with π light in both steps of the resonance fluorescence process. The phase reversal of the two signals is due to the sign reversal of the magnetic field.

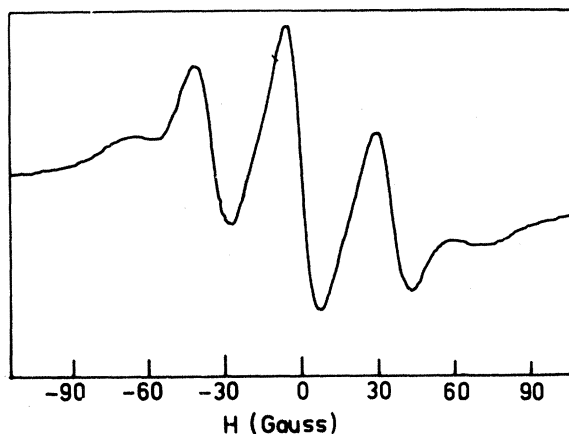


FIG. 4. Level-crossing signals obtained with an enriched sample of Yb^{173} . The incident (or detected) light was linearly polarized at an angle of 55° to the magnetic field direction. The detected (or incident) light was unpolarized.

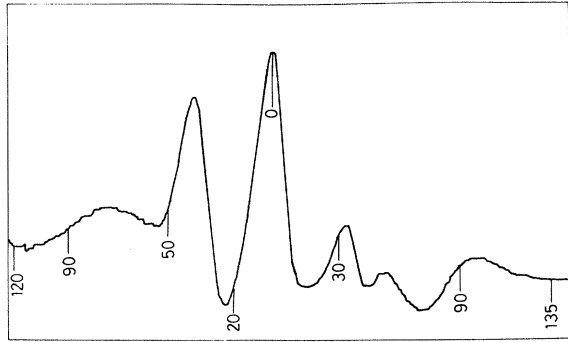


FIG. 5. Asymmetric level-crossing signals (labeled in gauss) observed with linearly polarized light at 55° to the z direction in both steps of the resonance fluorescence process.

the $\Delta m = 1$ signal, since θ of 55° becomes $\theta' = 125^\circ$ as the field sweeps through zero and $\sin 2\theta = -\sin 2\theta'$. The magnitude of the effect of the sign reversing $\Delta m = 1$ signal from an inspection of Fig. 5 is in good agreement with the predictions of Table II. Unfortunately no information regarding hfs can be obtained from the asymmetric curves.

The level crossing observed at $147.2(12)$ G can be used in conjunction with Eq. (1) to obtain the ratio $A^{171}/g_J = 206.0(16)$ Mc/sec. We have noted above that once the hfs constant A^{171} is determined, we may use the Fermi-Segre relation¹⁴

$$A^{171}/A^{173} = g_I^{171}/g_I^{173} \quad (4)$$

and the known ratio of the g_I factors⁸ to deduce a value for A^{173} . Thus we find $A^{173}/g_J = 56.9$ Mc/sec. Taking $g_J = 1.05$, we calculate $A^{173} = 59.7$ Mc/sec. The position of the level crossing at 36.2 G may be used to extract a value of B/A for Yb^{173} , the ratio of quadrupole to dipole hfs constants. We use the formula appropriate to $J = 1$ and $I = \frac{5}{2}$.

$$(3A/g_J)(1 + \frac{9}{40}b - \frac{9}{400}b^2) = \mu_0 H_c (1 + \frac{9}{40}b), \quad (5)$$

where $b = B/A$ and H_c is the crossing field.¹⁵ Higher-order terms are negligible at our level of precision. Alternatively, the $(F = \frac{7}{2}) \leftrightarrow (F = \frac{3}{2})$ hfs interval can be expressed as a linear combination of A and B . With A known, the interval as given by the anticrossing signal gives B directly. In practice both the crossing and anticrossing data were fed into a computer and, with A , g_J , and g_I held fixed, a least-squares-fit value of B was obtained. We find $B = 604(7) \times g_J/1.05$ Mc/sec, where the proportionality of B to g_J is noted explicitly.

It is important to note that neither the crossing nor the anticrossing signal measures the sign of the hfs interval. We therefore attempted to fit the data by inverting the $F = \frac{7}{2}$ and $F = \frac{3}{2}$ levels, holding A fixed at 59.7 Mc/sec, and varying B . We find $B = 983$ Mc/sec. This value is very far from the one quoted by Murakawa. Therefore we abandon it in preference to the noninverted value given

above which is in close agreement with Gerstenkorn's measurement.

DISCUSSION OF THE RESULTS

Breit and Wills¹⁶ have treated the problem of the hfs constants for the levels of an sp configuration. The hazard of attempting to predict the hfs constants of the 1P_1 level on the basis of data obtained for the 3P_2 and 3P_1 levels has recently been pointed out by Lurio.³ The discrepancy between theory and experiment is especially glaring in the case of cadmium. By allowing the radial parameter of the p electron, $\langle 1/r^3 \rangle$, to have different values in the singlet and triplet levels, Lurio attains a more satisfactory level of agreement. The predicted value for the sign of the magnetic dipole hfs constant for Cd^{111} now agrees with the measured sign although a significant discrepancy still exists for the magnitude of the constant.

The procedure for applying the modified Breit-Wills theory is as follows: The variation of the p -electron wave function in the singlet and triplet states is accounted for by the introduction of a parameter, λ , such that $\langle 1/r^3 \rangle_{SS} = \lambda^2 \langle 1/r^3 \rangle_{TT}$ where the superscripts stand for singlet and triplet states. In addition, a mixed parameter that arises from cross terms, $\langle 1/r^3 \rangle_{ST}$, is set equal to $\lambda \langle 1/r^3 \rangle_{TT}$. The purpose of introducing λ is to partially take into account the effects of configuration interaction. The λ can be calculated purely from a knowledge of the fine structure intervals. Auxiliary constants that are required for the calculation are: α and β , the intermediate coupling constants, ξ , η , and θ which arise from relativistic corrections to various radial matrix elements and are defined by Schwartz.¹⁷ The values we have chosen for these constants are 0.991 , -0.133 , 1.03 , 1.20 , and 1.60 , respectively. We are now in a position to extract the individual electron hfs constant, a_s and $a_{3/2}$, from the measured values of $A(^3P_2)$ and $A(^3P_1)$. The results of such a calculation are presented in Table III for the cases $\lambda = 1$ (old Breit-Wills theory) and $\lambda = 0.743$ (modified Breit-Wills theory). The two sets of

TABLE III. Comparison of experimental and calculated values of dipole and quadrupole interaction constants. The derived single-electron and predicted coupling constants in column three are those of the Breit-Wills theory. Column four lists these same constants as obtained using the modified Breit-Wills theory.

hfs constant	Experimental value (Mc/sec)	Calculated values (Mc/sec)	
		Breit-Wills $\lambda = 1$	Modified Breit-Wills $\lambda = 0.743$
$A(^3P_2)$	-737.7
$A(^3P_1)$	-1094.37
a_s	...	-2837	-2811
$a_{3/2}$...	-37.8	-46.5
$A(^1P_1)$	59.7	189	142
$B(^3P_2)$	-1313
$B(^3P_1)$	-826.58	-785	-785
$B(^1P_1)$	+604	912	489

constants can now be used to predict $A(^1P_1)$. The modified theory represents an improvement, although the absolute agreement is still poor.

The situation is far better for the quadrupole hfs constants. Since only one-single electron constant, $b_{3/2}$, is involved, it is identical to the measured value of $B(^3P_2)$. Both $B(^3P_1)$ and $B(^1P_1)$ can now be inferred for the two alternative values of λ . No difference is noted for $B(^3P_1)$. However, the measured value of $B(^1P_1)$ definitely favors the modified theory for which $\lambda = 0.743$.

The discrepancy in the case of the magnetic dipole interaction constant may have the following

explanation. Nir¹⁸ has attempted to fit the observed energy levels of the $(4f)^{14}6s6p$ and $(4f)^{13}5d(6s)^2$ configurations using Racah techniques. He finds that the 1P_1 level of $6s6p$ is only approximately 75% pure sp and contains considerable admixture of $f^{-1}d$. We have measured the hfs constant for the 3P_1 level of $f^{-1}d$.⁴ The magnitude of the A value for this level, its inferred sign, and the degree of admixture are precisely what is required to exactly reproduce the experimental value $A(^1P_1)$ for $6s6p$ although the agreement is to be considered fortuitous since other levels are admixed as well.

*This research has been sponsored in part by the Physics Branch, U.S. Office of Naval Research, Washington, D.C., under Contract No. F61052-67-C-0100.

†Present address: New York University, University Heights, New York.

¹J.S. Ross and K. Murakawa, J. Phys. Soc. Japan **19**, 249 (1964).

²S. Gerstenkorn, private communication.

³A. Lurio, Phys. Rev. **142**, 46 (1966).

⁴B. Budick and J. Snir, to be published.

⁵B. Budick and J. Snir, Phys. Rev. Letters **20**, 177, 701 (1968).

⁶T.G. Eck, L. L. Foldy, and H. Wieder, Phys. Rev. Letters **10**, 239 (1963).

⁷B. Budick and J. Snir, Phys. Letters **24B**, 276 (1967).

⁸L. Olschewski and E.W. Otten, Z. Physik **200**, 224

(1967).

⁹P.A. Franken, Phys. Rev. **121**, 508 (1961).

¹⁰W. Meggers, to be published.

¹¹H. Wieder and T.G. Eck, Phys. Rev. **153**, 103 (1967).

¹²B. Budick and L.A. Levin, in La Structure Hyperfine Magnetique des Atomes et des Molecules (Centre National de Recherche Scientifique, Paris, 1966).

¹³M. Baumann and G. Wandel, Phys. Letters **22**, 283 (1966).

¹⁴H. Kopfermann, Nuclear Moments (Academic Press, Inc., New York, 1958), p. 159.

¹⁵A. Landman and R. Novick, Phys. Rev. **134**, A56 (1964).

¹⁶G. Breit and L.A. Wills, Phys. Rev. **44**, 470 (1933).

¹⁷C. Schwartz, Phys. Rev. **97**, 380 (1955).

¹⁸S. Nir, private communication.